JOURNAL OF GEOPHYSICAL RESEARCH, VOL. 89, NO. B9, PAGES 7845-7851, SEPTEMBER 10, 1984

SHOCK TEMPERATURES IN CaO

Mark B. Boslough[1] and Thomas J. Ahrens

Seismological Laboratory, California Institute of Technology, Pasadena

Arthur C. Mitchell

Lawrence Livermore National Laboratory, Livermore, California

Abstract. Blackbody temperatures of CaO shocked to pressures from 140 to 182 GPa have been measured in the 3750 to 6000 K range using the Lawrence Livermore National Laboratory light gas gun. These shock temperatures, along with Hugoniot data for single crystal and porous CaO and isothermal data, are used to construct equations of state for the high pressure (B2) phase of CaO. The zero-pressure density of the B2 phase is between 3.8 and 4.0 Mg/m^3 and the B1-B2 transition energy is 2.1 to 2.3 MJ/kg. The density and bulk modulus at pressures from 70 to 135 GPa are similar to seismically determined values for the lower mantle of the earth. Thus the lower mantle could have a substantial inventory of Ca-bearing minerals, and mixed oxide models, for the composition of the lower mantle will be insensitive to the quantity of CaO assumed.

Introduction

The calcium-bearing minerals perovskite ($CaTiO_3$), melilite ($Ca_2Al_2SiO_7$-$Ca_2MgSi_2O_7$), diopside ($CaMgSi_2O_6$), and anorthite ($CaAl_2Si_2O_8$) may be among the first phases to condense from the solar nebula [Grossman and Larimer, 1974]. They are of geophysical importance because they are hosts for the actinide series elements U and Th and because Ca is the most common large-ion lithophile element in the solar system [Ross and Aller, 1976]. In inhomogeneous accretion models [Turekian and Clark, 1969] the lower mantle is significantly enriched in the chemical components derived from these minerals. At the high pressures of the lower mantle (70 to 135 GPa) these minerals transform into a series of high pressure phases [Liu, 1978, 1979] whose high pressure equation of state properties may be close to those of their equivalent mixed oxides [Boslough et al., unpublished manuscript, 1984]. Thus the high pressure behavior of CaO is of interest.

CaO exists in the B1 (NaCl) structure under standard conditions, and densities calculated by extrapolation of its compression curve [e.g. Perez-Albuerne and Drickamer, 1965; Chang and Graham, 1977; Mammone et al., 1981] to lower mantle pressures are significantly lower than seismologically determined lower mantle densities [e.g. Dziewonski et al., 1975; Anderson and Hart, 1976; Dziewonski and Anderson, 1981] (see also Figure 1). Jeanloz et al. [1979] found that at about 70 GPa, CaO undergoes a phase transition to the B2 (CsCl) structure, which is denser than the B1 structure phase. At high pressure the B2 phase of CaO has densities and compressibilities which, according to Hugoniot data [Jeanloz and Ahrens, 1980], are close to those of the mantle.

The reason for conducting shock temperature experiments on this material is to characterize its thermal properties at high pressures. Not only can the energetics of the B1-B2 phase transition be constrained, but the possible existence of further phase transitions in this pressure range, such as melting, can be determined. The temperature-pressure Hugoniot is much more sensitive to such transitions than is the pressure-density Hugoniot [Lyzenga et al., 1983]. Armed with well-constrained transition energies in this way, the adiabatic compression curve (K_{os} and K_{os}' in the Birch-Murnaghan approximation; Davies [1973]) can be determined with better precision.

Experimental Methods

The CaO samples were obtained from Oak Ridge National Laboratory where they were grown by an arc-fusion process. They are from the same boule as samples used by Jeanloz and Ahrens [1980] and are free from all but trace impurities. Ideally, samples should be perfectly transparent, as optical methods are used to determine the shock temperature. These samples appear bluish in color, and transmitted light is significantly yellowed. This is due to the Rayleigh scattering of white light, probably by microbubbles inherently present in highly pure crystals grown by the arc-fusion method [Abraham et al., 1971]. A Cary 17 spectrophotometer was used to measure the absorbance and scattering at visible and near infrared wavelengths [Figure 2]. It demonstrates an approximate λ^4 dependence, as is expected with Rayleigh scattering [Jackson, 1975].

There is some evidence for minute amounts of hydration in the form of portlandite ($Ca(OH)_2$) in infrared spectra [Jeanloz and Ahrens, 1980]. Both the microbubbles and the portlandite should lead to bulk densities which are lower than the X ray density. This is observed; densities of samples used range from 3.341 to 3.345 Mg/m^3, compared to the X ray density of 3.345 Mg/m^3. Samples were approximately 3 mm thick and 17 mm wide, and both surfaces were polished to optical quality. They were mounted on copper driver plates and shocked to pressures from 140 to 182 GPa by 2-mm-thick copper and tantalum flyer plates fired from the Lawrence Livermore Laboratory light gas gun [Mitchell and Nellis, 1981] at speeds from 6.3 to 7.1 km/s.

[1]Now at Sandia National Laboratories.

Paper number 4B0519.
0148-0227/84/004B-0519$05.00

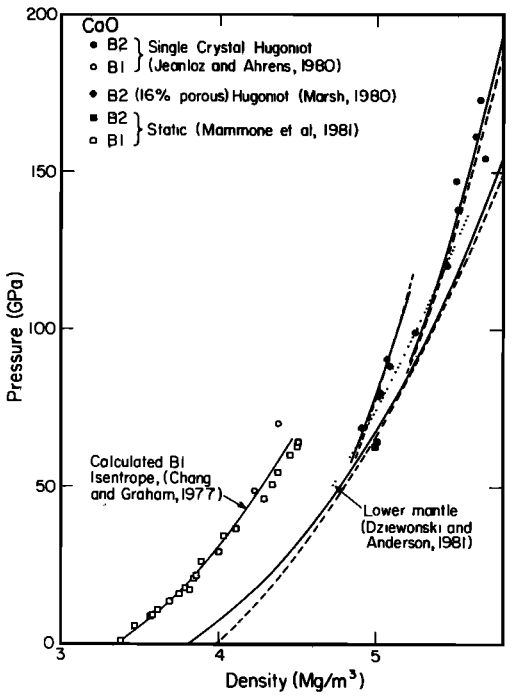

Fig. 1. Single crystal Hugoniot data [Jeanloz and Ahrens, 1980], porous CaO Hugoniot data [Marsh, 1980], and static isothermal data [Mammone et al., 1981] for CaO. Solid and dashed curves are low and high zero-pressure density fits to B2 data, respectively. Calculated B1 isentrope based on ultrasonically determined values of K_{OS} = 112.5 GPa and K'_{OS} = 4.8, of Chang and Graham [1977]. Lower mantle curve based on PREM model of Dziewonski and Anderson [1981].

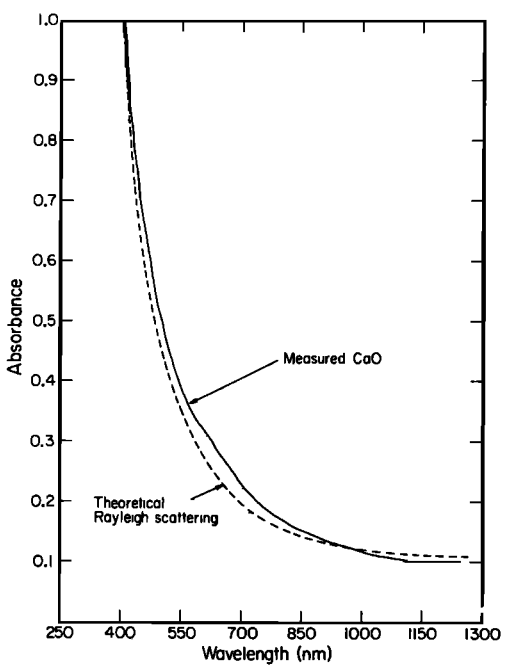

Fig. 2. Absorbance spectrum of a representative sample of CaO, measured with Cary 17 Spectrophotometer. Theoretical curve is of form: $[h_o (\lambda_o/\lambda)^4 + \mu]d$ with $h_o d_o = 0.9$, $\mu d_o = 0.1$, and $\lambda_o = 400$ nm.

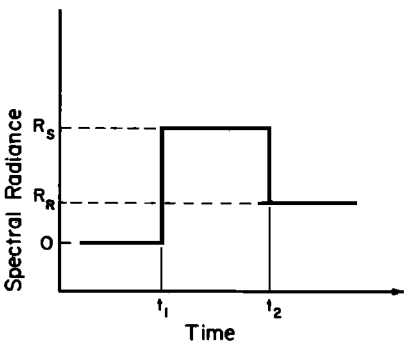

Fig. 3. Hypothetical shock temperature record for ideal case where initial state is perfectly transparent and shock state is perfect blackbody. Shock wave enters sample at time t_1 and reaches free surface at t_2. R_S and R_R are spectral radiances characteristic of shock temperature and postshock temperature, respectively.

The projectile velocity was determined by flash radiography and this was used in an impedance match solution [Rice et al., 1958] to calculate the shock pressure in the CaO. Thermal radiation was emitted from the shocked material and transmitted through the unshocked portion of the sample, which acts as a window. The intensity of the light was measured at six wavelengths in the visible and near infrared with an optical pyrometer [Lyzenga and Ahrens, 1979]. The measured spectral radiances were used to calculate the shock temperature.

Results and Discussion

In an ideal situation in which the sample is initially perfectly transparent, the shocked sample is perfectly opaque, and the shock wave is planar, parallel to the sample faces, and exhibits no time-dependent behavior, the shock-induced radiance versus time profile would appear as in Figure 3. At time t_1 the shock wave enters the transparent sample from the opaque driver plate. The shocked material immediately begins to radiate at an intensity determined by its temperature, and the signal increases suddenly to R_S. As the shock wave approaches the free surface, it is steady, so the signal is constant. At time t_2 the shock reaches the free surface and reflects as a rarefaction wave. The light intensity drops to R_R, characteristic of the residual, postshock temperature.

A typical shot record from this study is shown in Figure 4. It deviates from the ideal case in two principal ways. First, the rise from t_a to t_b is not instantaneous but is nearly 50 ns. Second, the light intensity is not constant during shock transit but increases approximately linearly with time.

The long rise time from t_a to t_b cannot be accounted for by the HP5082-4207 photodiode rise time, which is approximately 1 ns [Lyzenga and Ahrens, 1979], nor is it due to shock wave tilt within the field of view of the photodiode. The active area of the detector is about 1 mm in diameter, and the optics demagnify the image by a factor of 0.43, so the field of view is 2.3 mm. The maximum projectile tilt is 0.05 radians [Mitchell and Nellis, 1981]. At typical

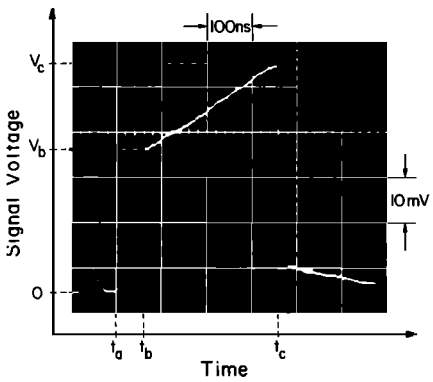

Fig. 4. Shock temperature record for shot CaO3T at λ = 508 nm. Time t_a: shock wave enters sample, light is scattered indirectly to detector. Time t_b: shock wave enters detector field of view. Time t_c: shock wave reaches free surface; spectral radiance is read at this point.

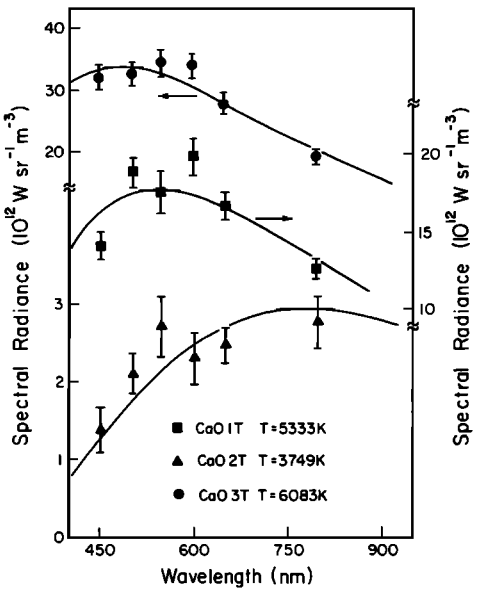

Fig. 5. Spectral radiance data for three shots, with best fitting blackbody curves.

projectile velocities of 6 mm/μs the maximum time interval for the line of intersection between shock front and driver/sample interface to cross the field of view is 20 ns, insufficient to account for the measured time lag. As the samples are strong optical scatterers, the material within the detector field of view begins scattering light from the shock wave the instant it enters at one edge of the sample. The line of intersection between shock front and driver/sample interface can take as long as 70 ns to sweep across the 8 mm from the sample edge into the photodetector field of view, accounting for the long observed rise times. Unfortunately, interference from this scattered light precludes precise determination of the shock transit times, so these experiments cannot be used to determine Hugoniot states (e.g. Boslough et al., unpublished manuscript [1984] for anorthite glass).

The approximately linear increase in light intensity with time as the shock wave propagates through the sample can be explained by scattering and absorption of light. The intensity of light transmitted through a medium is decreased by a factor of $e^{-(\mu+h)d}$, where μ is the linear absorption coefficient, h is the extinction coefficient due to scattering, and d is the light propagation distance through the medium. This distance is $(t_c-t)U_s$, where U_s is the shock velocity, t is time, and t_c is the time of shock arrival at the free surface. As the shock wave approaches the free surface the light intensity is approximately

$$I = I_o\,[1 - (\mu + h)(t_c - t)U_s] \qquad (1)$$

which increases linearly with time, where I_o is the intrinsic radiated (unattenuated) intensity. At $t = t_c$ the measured intensity is equal to the radiated intensity, so shot records were read at free surface arrival t_c. The spectral radiances determined in this way, along with their uncertainties, are given in Table 1 and plotted in Figure 5.

The ratio of initial intensity I_b to final intensity I_c was found to be smaller at shorter wavelengths, consistent with Rayleigh scattering. In Table 2, measured values are tabulated for shot CaO3T, along with the best fitting theoretical values, which assume a wavelength dependent Rayleigh scattering component $h = h_o\,(\lambda_o/\lambda)^4$ and a wavelength independent absorption component μ. The effects of the two sources of attenuation are about equal at λ=450 nm and the wavelength independent component dominates at λ=792 nm.

TABLE 1. Calcium Oxide Spectral Radiance Data

λ, nm	N_λ, 10^{12} W m^{-3} Sr^{-1}		
	CaO2T	CaO1T	CaO3T
450.2	1.38±0.30	13.9±0.9	32.1±2.1
507.9	2.11±0.25	18.6±1.0	32.4±2.0
545.1	2.72±0.38	17.3±1.4	34.2±2.3
598.0	2.31±0.33	19.6±1.2	33.7±2.0
650.0	2.47±0.23	16.4±0.9	27.8±1.6
792.0	2.78±0.34	12.3±0.6	18.9±1.2

Shock Temperatures

Two approaches were used to determine shock temperatures from optical pyrometer shot records.

TABLE 2. Shot CaO3T Measured and Theoretical Intensity Ratios

λ, nm	$\xi_{measured}$	$\xi_{theoretical}$
450	0.56	0.56
508	0.46	0.46
545	0.37	0.41
598	0.42	0.37
650	0.37	0.35
792	0.29	0.32

$\xi_{measured} = -\ln\,(I_b/I_c)$; $\xi_{theoretical} = [\mu + h_o(\lambda_o/\lambda)^4]d_o$; $h_o d_o = 0.27$, $\mu d_o = 0.29$ (best fit to data); $\lambda_o = 450$ nm.

TABLE 3. Calcium Oxide Shock Temperature Data

Shot	Flyer/Driver Material	Projectile Velocity, km/s	Initial Density, Mg/m^3	Pressure, GPa	Temperature Calculation				
					Method	ϵ	T K	σ, W/sr m^3	$\sigma/\overline{N}_\lambda$
CaO2T	Cu/Cu	6.258±0.055	3.3449±0.0013	140.1±1.9	a	0.60	4075±156	5.8×10^{11}	0.25
					b	1.00	3749±178	7.8×10^{11}	0.34
CaO1T	Cu/Cu	7.102±0.021	3.3422±0.0012	171.0±1.2	a	1.09	5242±222	3.4×10^{12}	0.21
					b	1.00	5333±238	3.5×10^{12}	0.21
CaO3T	Ta/Cu	6.457±0.027	3.3411±0.0014	181.6±1.2	a	1.15	5899±195	4.2×10^{12}	0.14
					b	1.00	6083±225	4.5×10^{12}	0.15

Method a: best fit with Planck function and variable ϵ. Method b: best fit with Planck function and $\epsilon \equiv 1$ (blackbody).

Both involve least squares fitting the spectral radiance data to a Planck distribution function [Boslough, 1983]. In method a, both the emissivity and temperature are varied to obtain the best fit. In method b, only the temperature is allowed to vary; the emissivity is taken as unity, equivalent to the assumption of a blackbody.

Temperatures and emissivities calculated via methods a and b are presented in Table 3, with the standard deviations σ and mean fractional deviations $\sigma/\overline{N}_\lambda$, where $\overline{N}_\lambda$ is the mean measured spectral radiance. Pressures are calculated from an impedance match solution using the measured impact velocity and the known Hugoniots of the flyer materials [McQueen et al., 1970] and CaO [Jeanloz and Ahrens, 1980]. In two of the three experiments the emissivities which lead to the best fit are greater than unity: an unphysical situation. In all experiments, method a does not give significantly better agreement than method b, as measured by the standard deviation. Shot CaO2T was the only experiment which led to a best fit with $\epsilon < 1$. If the emissivity were really 0.6, as determined by the fit, one would expect to see the time-dependent behavior similar to that observed in forsterite by Ahrens et al. [1982] or in anorthite glass at lower pressures by Boslough [1983]. For emissivities well below unity an approximately exponential decaying signal is seen soon after entry of the shock wave into the sample. This is caused by the increasing thickness of the absorbing layer of shocked material between the detector and the radiating driver-sample interface, which is heated to high temperature by the closing of the gap between the two materials. This phenomenon is described in detail by Boslough [1983]. Because this is not observed, it is reasonable to conclude that the emissivity is close to unity for all three experiments. Blackbody curves corresponding to temperatures determined in this way are plotted with the radiance data in Figure 5.

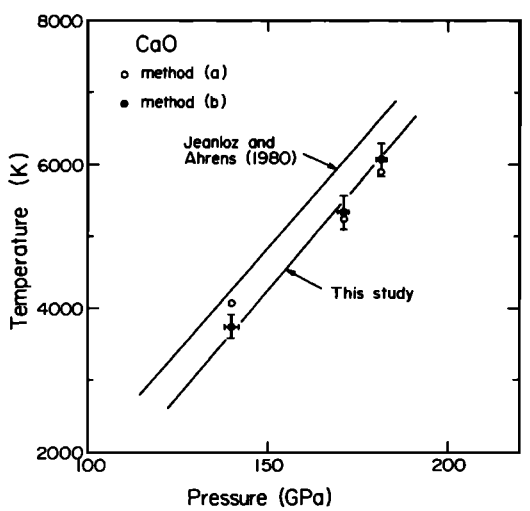

Fig. 6. Shock temperature data determined by method a ($\epsilon \neq 1.0$) and method b (blackbody). Calculated Hugoniots based on Jeanloz and Ahrens [1980] and both low and high zero-pressure density solutions of this paper (which are identical in the P-T plane).

Why alkaline earth oxides such as CaO and MgO [Svendsen and Ahrens, 1983] should behave approximately as blackbodies when shocked to these pressures is not understood in detail. This type of behavior has been observed in other initially transparent molecular and ionic materials shocked to pressures of the order of 100 GPa. Emissivities greater than 0.9 have been observed in shocked quartz [Lyzenga et al., 1983], NaCl [Ahrens et al., 1982], water [Lyzenga et al., 1982], polybutene [Nellis et al., 1984], and anorthite glass [Boslough et al., unpublished manuscript, 1984]. This is expected, as most materials, particularly those which undergo phase transformations, become opaque when shocked to pressures above 100 GPa. Possible mechanisms are discussed by Kormer [1968] and Lyzenga [1982]. These include high densities of defects such as color centers and exitation of electrons into the conduction band by the high temperatures.

Equation of State

Shock temperatures determined by methods a and b are plotted in the P-T plane in Figure 5, along with a theoretical calculation by the method of Ahrens et al. [1969], based on parameters of Jeanloz and Ahrens [1980], and a Dulong-Petit specific heat $C_v = 3R$. The temperatures calculated by method a, if taken at face value, could be interpreted as indicating a minor phase transition at about 4000 K, because as the shock pressure increases, the measured shock temperature

decreases significantly with respect to the calculated P-T Hugoniot of a single phase. Calculations based on this temperature offset give a transition energy $E_{tr} > 0.5$ MJ/kg. We do not favor this interpretation, because we prefer temperature calculated by method b, but include it for completeness. The results of method b (blackbody temperatures) are preferred for reasons outlined above. On this basis there is no evidence for a phase transition at or above 4000 K. However, all three measured temperatures lie about 600 K below the theoretical curve of Jeanloz and Ahrens [1980], indicating that E_{tr}, the energy of transition between the initial state and the metastable final phase at standard conditions, is actually larger than the value used in the earlier calculations: 1.6 MJ/kg.

One possible interpretation is a second phase transition below 140 GPa. This phase transition would have to have an $E_{tr} \sim 0.5$ MJ/kg, unless E_{tr} for the B1 to B2 transition is significantly less than 1.6 MJ/kg, which is unlikely. Such a small E_{tr} would probably not result from melting, which would be expected to have an E_{tr} of around 1.4 MJ/kg, the latent heat of fusion at 1 atmosphere [Robie et al., 1979]. There is no evidence for such a phase transition from the Hugoniot data of Jeanloz and Ahrens [1980].

If the B2 phase indeed exists on the Hugoniot to 182 GPa, a complete equation of state for that phase can be constructed from the present data. Rather than simply assuming the parameters determined by Jeanloz and Ahrens [1980] and finding the E_{tr} which provided the best agreement to the new temperature data, all the available data for the B2 phase were simultaneously fit. This included porous CaO Hugoniot data [Marsh, 1980] and isothermal data [Mammone et al., 1981]. The inversion procedure was based on third order finite strain theory [Davies, 1973] and the Mie-Gruneisen approximation, with γ/V assumed constant, where γ is the thermodynamic Gruneisen parameter $V(\partial P/\partial E)_V$. First, a zero-pressure density of the B2 phase was assumed, and the least squares method of Vassiliou and Ahrens [1981] was used to determine the bulk modulus K_{os} and its first pressure derivative dK_s/dP, based on all data in the P-ρ plane. The Gruneisen parameter γ_o was varied to optimize the fit. We found that the fit improved with increasing γ_o, even to unphysically large values, so we stopped increasing it when it reached 1.8, the large value used by Jeanloz and Ahrens [1980]. Finally, the above procedure was repeated using different values of E_{tr}, until the value which gave the best agreement to the P-T data was found. The entire procedure was carried out for a whole range of zero-pressure densities. This inversion method is admittedly nonunique in that the zero-pressure density of the B2 phase is not well constrained; however, it can be held within values which lead to physically reasonable values for the other parameters. Despite the abundance of data, a wide range of values provided good conformity. Parameters for the two extreme models are given in Table 4, based on zero-pressure densities of 3.8 and 4.0 Mg/m^3. One salient feature evident from the table is that $E_{tr} = 2.2 \pm 0.1$ MJ/kg is nearly model independent, so its value is constrained to better than ±5%.

Curves calculated with these parameters are plotted with the shock temperature data in Figure 5 and with the isothermal and Hugoniot data in Figure 1. Both the low- and high-density solutions give approximately the same curve in the P-T plane, but the high density equation of state requires a 0.2 MJ/kg greater energy of transition. The slope of the theoretical curve is determined primarily by the specific heat. It is in good agreement with the data, indicating that the Dulong-Petit value ($C_V = 3R$) is a good approximation for CaO, in contrast to the situation for the high pressure phases of anorthite [Boslough, 1983] and quartz [Lyzenga et al., 1983].

TABLE 4. Fits to CaO B2 Data

	Low-Density Fit	High-Density Fit
ρ, Mg/m^3	3.8	4.0
K_{os}, GPa	121.0	190.0
dK_s/dP	5.2	4.0
E_{tr}, MJ/kg	2.1	2.3
γ_o	1.8	1.8

Application to the Earth

The theoretical curves in the P-ρ plane can be compared to the lower mantle curve [Dziewonski and Anderson, 1981] in Figure 1. At 130 GPa (a pressure near that at the base of the lower mantle) the temperature on the Hugoniot of CaO is about 3100 K, which is very close to Stacey's [1977] geotherm. At this point, densities can be compared directly, and the mantle is denser by up to 1%. In order to compare CaO to the geotherm at other pressures, a thermal correction must be made. When this is done, the CaO curve is still found to be steeper in the P-ρ plane than the mantle curve but less steep than the Hugoniot, and at lower pressures the densities are closer. Similarly, the adiabatic bulk modulus of CaO in this pressure range was found to be from 3 to 13% greater than that of the lower mantle. If the shock temperature and Hugoniot data above 140 GPa correspond to a post-B2 phase, this phase would still be well described by the equation of state presented here for the B2 phase and the close comparisons of both ρ and K to the lower mantle are still valid. However, because it would be based only on the data above the hypothetical post-B2 phase transition pressure it would not be as well constrained. The transition energy between this phase and the B1 phase would still be well constrained, however, because it is strongly dependent on the measured shock temperatures.

Conclusions

The first shock temperature data have been presented for CaO to 182 GPa. As there is no strong evidence for a post-B2 phase transition in CaO below 182 GPa from either Hugoniot or shock-temperature data, we believe these data correspond to CaO in the B2 structure. They can be fit well with theoretical shock temperature

calculations for CaO in the B2 phase and allow a precise energy of transition (2.1 to 2.3 MJ/kg at STP) to be determined for the B1-B2 phase transformation. This E_{tr} in turn provides further constraint for calculating the bulk modulus and its pressure derivative from Hugoniot data. A range of equations of state were determined in this manner. The equation of state with the lowest zero-pressure density in the range does not differ greatly from that of Jeanloz and Ahrens [1980] but is better constrained. At lower mantle pressures the present models predict densities of CaO to be lower than the lower mantle [Dziewonski and Anderson, 1981] by up to 1% and bulk moduli to be greater by 3 to 13%. Thus depending on the bulk properties of the other components of lower mantle models, and the particular model used, CaO cannot be precluded as a major component of the lower mantle on the basis of its density and bulk modulus. However, because such a wide range of equations of state for the B2 phase are indistinguishable with the data, theoretical considerations may be necessary to choose the best equation of state.

Acknowledgments. We wish to thank D. Bakker, E. Jerbic, and the rest of the technical personnel at the Lawrence Livermore National Laboratory light-gas gun facility and standards laboratory. We appreciate discussions with G. Lyzenga, W. Nellis, and J. Trainor, and the facilities provided by W. Nellis at Livermore. M. Abraham provided CaO samples, and G. Rossman and his students at Caltech provided assistance in determining optical properties, for which we are grateful. We also appreciate the help of E. Gelle and others at the Caltech shock-wave laboratory in sample preparation. Support was provided by National Science Foundation grant EAR78 12942 at the California Institute of Technology and by the Lawrence Livermore National Laboratory. This is contribution 3931 from the Division of Geological and Planetary Sciences, California Institute of Technology.

References

Abraham, M. M., C. T. Butler, and Y. Chen, Growth of high-purity and doped alkaline earth oxides, 1. MgO and CaO, J. Chem. Phys., 55, 3752-3756, 1971.

Ahrens, T. J., C. F. Peterson, and J. T. Rosenberg, Shock compression of feldspars, J. Geophys. Res., 74, 2727-2746, 1969.

Ahrens, T. J., G. A. Lyzenga, and A. C. Mitchell, Temperatures induced by shock waves in minerals: Applications to geophysics, in High-Pressure Research in Geophysics, edited by S. Akimoto and M.H. Manghnani, pp. 579-594, Center for Academic Publications Japan, Tokyo, 1982.

Anderson, D. L., and R. S. Hart, An earth model based on free oscillations and body waves, J. Geophys. Res., 81, 1461-1475, 1976.

Boslough, M. B., Shock-wave properties and high-pressure equations of state of geophysically important materials, Ph.D. Thesis, Calif. Inst. of Technol., Pasadena, 1983.

Chang, Z. P., and E. K. Graham, Elastic properties of oxides in the NaCl-structure, J. Phys. Chem. Solids, 38, 1355-1362, 1977.

Davies, G. F., Quasi-harmonic finite strain equations of state of solids, J. Phys. Chem. Solids, 34, 1417-1429, 1973.

Dziewonski, A. D., and D. L. Anderson, Preliminary reference earth model, Phys. Earth Planet. Inter., 25, 297-356, 1981.

Dziewonski, A. M., A. L. Hales, and E. R. Lapwood, Parametrically simple earth models consistent with geophysical data, Phys. Earth Planet. Inter., 10, 12-48, 1975.

Grossman, L., and J. W. Larimer, Early chemical history of the solar system, Rev. Geophys. Space Phys., 12, 71-101, 1974.

Jackson, J. D., Classical Electrodynamics, John Wiley, New York, 1975.

Jeanloz, R., and T. J. Ahrens, Equations of state of FeO and CaO, Geophys. J. R. astron. Soc., 62, 505-528, 1980.

Jeanloz, R., T. J. Ahrens, H. K. Mao, and P. M. Bell, B1/B2 transition in CaO from shock-wave and diamond cell experiments, Science, 266, 829-830, 1979.

Kormer, S. B., Optical study of the characteristics of shock-compressed condensed dielectrics, Sov. Phys. Usp. Engl. Transl., 11, 229-254, 1968.

Liu, L.-G., A new high-pressure phase of $Ca_2Al_2SiO_7$ and implications for the earth's interior, Earth Planet. Sci. Lett., 40, 401-406, 1978.

Liu, L.-G., High-pressure phase transformations in the system $CaSiO_3$-Al_2O_3, Earth Planet. Sci. Lett., 43, 331-335, 1979.

Lyzenga, G. A., Optical pyrometry at high shock pressures and its interpretation, in Shock Waves in Condensed Matter-1981, edited by W. J. Nellis, L. Seaman, and R. A. Graham, pp. 268-276, American Institute of Physics, New York, 1982.

Lyzenga, G. A., and T. J. Ahrens, A multi-wavelength optical pyrometer for shock compression experiments, Rev. Sci. Instrum., 50, 1421-1424, 1979.

Lyzenga, G. A., T. J. Ahrens, W. J. Nellis, and A. C. Mitchell, The temperature of shock-compressed water, J. Chem. Phys., 76, 6282-6286, 1982.

Lyzenga, G. A., T. J. Ahrens, and A. C. Mitchell, Shock temperatures of SiO_2 and their geophysical implications, J. Geophys. Res., 88, 2431-2444, 1983.

Mammone, J. F., H. K. Mao, and P. M. Bell, Equations of state of CaO under static pressure conditions, Geophys. Res. Lett., 8, 140-142, 1981.

Marsh, S. P., LASL Shock Hugoniot Data, University of California Press, Berkeley, 1980.

McQueen, R. G., S. P. Marsh, J. W. Taylor, J. N. Fritz, and W. J. Carter, The equation of state of solids from shock wave studies, in High-Velocity Impact Phenomena, edited by R. Kinslow, pp. 293-417, Academic, New York, 1970.

Mitchell, A. C., and W. J. Nellis, Diagnostic system of the Lawrence Livermore National Laboratory two-stage light-gas gun, Rev. Sci. Instrum., 52, 347-359, 1981.

Nellis, W. J., F. H. Ree, R. J. Trainor, A. C. Mitchell, and M. B. Boslough, Equation of state and optical luminosity of benzene,

polybutene, and polyethylene shocked to 210 GPa (2.1 Mbar), J. Chem. Phys., 80, 2789-2799, 1984.

Perez-Albuerne, E. A. and H. G. Drickamer, Effect of high pressures on the compressibilities of seven crystals having the NaCl or CsCl structure, J. Chem. Phys., 43, 1381-1387, 1978.

Rice, M. H., R. G. McQueen, and J. M. Walsh, Compressibility of solids by strong shock waves, Solid State Phys., 6, 1-63, 1958.

Robie, R. A., B. S. Hemingway, and J. R. Fisher, Thermodynamic Properties of Minerals and Related Substances at 298.15K and 1 Bar (10^5 Pascals) Pressure and at Higher Temperatures, pp. 216-221, Government Printing Office, Washington, D. C., 1979.

Ross, J. E. and L. H. Aller, The chemical composition of the sun, Science, 191, 1223-1229, 1976.

Stacey, F. D., A thermal model of the earth, Phys. Earth Planet. Inter., 15, 341-348, 1977.

Svendsen, B. and T. J. Ahrens, Shock-induced radiation and temperatures of MgO (abstract), Eos Trans. AGU, 64, 848, 1983.

Turekian, K. K., and S. P. Clark, Jr., Inhomogeneous accretion model of the earth from the primitive solar nebula, Earth Planet. Sci. Lett., 6, 346-348, 1969.

Vassiliou, M. S., and T. J. Ahrens, Hugoniot equation of state of periclase to 200 GPa, Geophys. Res. Lett., 8, 729-732, 1981.

T. J. Ahrens, Seismological Laboratory 252-21, California Institute of Technology, Pasadena, CA 91125.

M. B. Boslough, Sandia National Laboratories, Division 1131, Albuquerque, NM 87185.

A. C. Mitchell, Lawrence Livermore National Laboratory, L-355, P. O. Box 808, Livermore, CA 94550.

(Received July 11, 1983;
revised February 22, 1984;
accepted March 30, 1984.)